Numerical Investigation on the Boundary Conditions for the Multiscale Base Functions

Shan Jiang[1] and Yunqing Huang[2,*]

[1] *Department of Mathematics, Xiangtan University, Xiangtan 411105, China.*
[2] *Hunan Key Laboratory for Computation and Simulation in Science and Engineering, Institute for Computational and Applied Mathematics, Xiangtan University, Xiangtan 411105, China.*

Abstract. We study the multiscale finite element method for solving multiscale elliptic problems with highly oscillating coefficients, which is designed to accurately capture the large scale behaviors of the solution without resolving the small scale characters. The key idea is to construct the multiscale base functions in the local partial differential equation with proper boundary conditions. The boundary conditions are chosen to extract more accurate boundary information in the local problem. We consider periodic and non-periodic coefficients with linear and oscillatory boundary conditions for the base functions. Numerical examples will be provided to demonstrate the effectiveness of the proposed multiscale finite element method.

1 Introduction

Many multiscale problems are often described by partial differential equations (PDEs) with highly oscillating coefficients. In practice, the coefficients may contain many scales spanning over a great extent [3]. On one hand, the direct use of traditional numerical methods, such as standard finite element method (FEM) or finite difference method (FDM), to the multiscale problems is very difficult since the mesh size has to be extremely small. On the other hand, the main interest is to acquire the large scale solution with accuracy instead of finding the small scale characters in detail. The multiscale finite element

---

Corresponding author. Email addresses: `shanjiang1980@gmail.com` (S. Jiang), `huangyq@xtu.edu.cn` (Y. Huang)

method (MFEM), whose goal is to obtain the large scale solution accurately and efficiently, is to capture large scale information by constructing the multiscale finite element base functions. This can be achieved by solving the base functions from the local problem in the elements. With proper boundary conditions, the base functions are adaptive to the features of the differential operator.

To capture the large scale solutions without resolving the small scale details, Babuška & Osborn [2] (for one-dimensional problems) and Babuška et al. [1] (for special two-dimensional problems) presented the generalized finite element method by introducing modified base functions that are based on the differential operator. Hou & Wu [12] extended the idea of [1, 2] and proposed the multiscale finite element method by solving the local homogenization problems for the base functions. Hou et al. [13] and Efendiev & Wu [8] provided many theoretical analysis and numerical experiments for the MFEM. Engquist & Luo [9] studied the convergence of the multigrid method for highly oscillatory elliptic problems on a new coarse-grid finite difference scheme. Huang & Xu [14,15] applied the partition of unity method (PUM) to the multiscale problems with highly oscillating coefficients, and proved that the PUM admitted optimal convergence rate with nonmatching and overlapping grids. In [4], Chen & Cui constructed a special multiscale rectangular element space whose base functions consisting of bilinear functions and bubble-like functions. In [5], Chen & Hou proposed a mixed multiscale finite element method with an over-sampling technique, which solves the local Neumann boundary value problem for the bases. Chen & Yue [6] considered the oversampling multiscale finite element method with a new upscaling technique for resolving the well singularities. Jenny et al. [16] and He & Ren [11] applied the multiscale finite volume method in subsurface flow simulation and for solving the ground-water flow problems, respectively. Ren & E [19] and Yue & E [20] studied the heterogeneous multiscale method for the modeling of complex fluids with application to two-phase porous media flow. In [17], Ming & Yue presented an overview of the recent development on the multiscale numerical methods. Efendiev & Hou [7] discussed the applications of the MFEM to two-phase immiscible flow simulation in which limited global information is taken into account, and the applications to inverse problems are also discussed. Nassehi et al. [18] developed the MFEM using bubble functions thus obtained stable solutions without excessive mesh refinement near the wall. In [10], a systematic review to the heterogeneous multiscale method (HMM), including the fundamental designing philosophy and the error analysis, is presented. Yue & E [21] systematically investigated the issues in the multiscale modeling, and discussed the mixed Dirichlet-Neumann boundary condition in porous media.

An advantage of the multiscale finite element method is that it can reduce the size of computation. For example, let N be the number of elements in each spatial direction, and let M be the number of subcell elements in each direction for solving the base functions. Then there are a total of $(MN)^d$ (d is the dimension) elements at the fine grid level. For the FEM, the computer memory required to solve the problem at the fine grid is $\mathcal{O}(M^d N^d)$, in contrast with the MFEM which requires only $\mathcal{O}(M^d + N^d)$ amount of memory. Moreover,

it should be noted that the MFEM solves the problem at the coarse mesh level $h = 1/N$, while the FEM solves the problem at the fine mesh level $h_s = h/M$. Even with coarser meshes, the MFEM can still obtain accurate solution, and is even more accurate than that of the much costing FEM in some cases [12].

This paper is organized as follows. The formulation of the two-dimensional multiple scales elliptic problem and the multiscale finite element method are given in Section 2. In Section 3, we consider two kinds of boundary conditions for the base functions in the local problem. Section 4 is concerned with the applications of the linear and the oscillatory boundary condition of the base functions in numerical experiments. Section 5 provides some concluding remarks.

2 Formulations of the multiscale problem

In this section, we introduce the model problem and the multiscale method. First, we state some notations and conventions to be used in this paper. The Einstein summation convention is used: summation is taken over repeated indices. Throughout the paper, we shall use the notations of standard Sobolev spaces and related norms. $L^2(\Omega)$ denotes the space of square integrable functions defined in domain Ω,

$$H_0^1(\Omega) = \{v \in H^1(\Omega); v = 0 \text{ on } \partial\Omega\}, \quad H_0^2(\Omega) = \{v \in H^2(\Omega); v = 0, \nabla v = 0 \text{ on } \partial\Omega\},$$

$H^{-1}(\Omega)$ is the dual of $H_0^1(\Omega)$. Moreover, C and C_i denote generic positive constants, which are independent of ε and h. For simplicity, we assume that Ω is an open unit square domain in R^2, i.e., $\Omega = (0,1)^2$, which satisfies the convexity assumption needed to obtain certain regularity properties for the elliptic operator.

2.1 Model problem

Consider the following second order elliptic equation:

$$\begin{cases} L_\varepsilon u_\varepsilon = f & \text{in} \quad \Omega, \\ u_\varepsilon = g & \text{in} \quad \partial\Omega, \end{cases} \tag{2.1}$$

where f is some smooth function in $L^2(\Omega)$, and the Dirichlet boundary condition g is defined on the domain,

$$L_\varepsilon = -\nabla \cdot (a_\varepsilon \nabla)$$

is the elliptic differential operator, ε is assumed to be small parameter, $a_\varepsilon = (a_{ij}^\varepsilon(\mathbf{x}))$ is the conductivity tensor and is a symmetric matrix which satisfies the uniform ellipticity condition:

$$\alpha |\xi|^2 \leq \xi_i a_{ij}^\varepsilon \xi_j \leq \beta |\xi|^2, \quad \forall \xi \in R^2$$

for some positive constants $0 < \alpha < \beta$.

In practice, a_ε may be highly oscillating or random, thus the solution u_ε displays a multiscale nature. For the case of conduction problem, (2.1) is the heat/electrical equation

through the composite materials, in which a_ε is the thermal/electric conductivity, and u_ε represents the temperature/electric potential. For the case of flow simulation, (2.1) is the pressure equation through the porous media, in which a_ε is the ratio of the permeability and the fluid viscosity, and u_ε represents the pressure. In these problems the multiscale nature comes from the highly oscillating coefficients

$$a_{ij}^\varepsilon(\mathbf{x}) = a_{ij}(\mathbf{x}, \frac{\mathbf{x}}{\varepsilon_k}), \tag{2.2}$$

where $\mathbf{x}$ denotes the two-dimensional spatial coordinates $\{x,y\}$, ε_k denotes several small positive parameters. For simplicity of notation we use u instead of u_ε, keeping in mind that u depends on ε_k in fact. It is known the multiple scales in the solution, which is the main difficulty, exist in both steady problem and transient problem. In this work, we only consider the steady problem in this paper.

The variational formulation of (2.1) is to seek $u \in H_0^1(\Omega)$ such that

$$a(u,v) = f(v), \quad \forall v \in H_0^1(\Omega), \tag{2.3}$$

where

$$a(u,v) = \int_\Omega a_{ij} \frac{\partial u}{\partial x_i} \frac{\partial v}{\partial x_j} d\mathbf{x}, \quad f(v) = \int_\Omega f v d\mathbf{x}, \quad i,j = 1,2. \tag{2.4}$$

It is easy to see that the bilinear form $a(u,v)$ is elliptic and continuous, i.e.,

$$C_1 |v|_{1,\Omega}^2 \le a(v,v) \le C_2 |v|_{1,\Omega}^2, \quad \forall v \in H_0^1(\Omega),$$
$$|a(u,v)| \le C |u|_{1,\Omega} |v|_{1,\Omega}, \quad \forall u,v \in H_0^1(\Omega).$$

Let $\mathcal{K}^h$ be a partition of Ω by rectangles K with mesh size h, $0 < h \ll 1$. In each element $K \in \mathcal{K}^h$, we define a set of nodal base $\{\phi^i, i = 1, \cdots, d\}$ with $d=4$ being the number of nodes of the rectangular element. Let $\mathbf{x}_j \in \bar{K}$ $(j = 1, \cdots, 4)$ be the nodal points of K and four nodal points labeled counterclockwise from the lower left corner as (x_1,y_1), (x_2,y_2), (x_3,y_3), (x_4,y_4).

2.2 The multiscale finite element method

The main difference between the MFEM and the FEM is *the construction of the base functions.* In the MFEM, the base functions ϕ^i are constructed with respect to the differential operator in the local problem and satisfy

$$\begin{cases} L_\varepsilon \phi^i = 0 & \text{in} \quad K \in \mathcal{K}^h, \\ \phi^i = \theta^i & \text{on} \quad \partial K. \end{cases} \tag{2.5}$$

We require $\phi^i(\mathbf{x}_j) = \delta_{ij}$, where δ_{ij} is the Kronecker symbols. To guarantee the well-posedness of the local problem (2.5), we should specify the boundary condition θ^i on ∂K, and the use of the different boundary conditions are crucial to the model problem [12, 21]. It is

required that the base functions ϕ^i are adaptive to the local property of the differential operator. As a consequence, the small scale information in each element K is taken into the large scale solution through the base functions.

The multiscale finite element method is accomplished by restricting the variational formulation (2.3) into a finite dimensional subspace of $H_0^1(\Omega)$, denoted by V^h. We assume that the base functions are continuous across the boundaries of the elements, so that

$$V^h = span\{\phi_K^i : i=1,\cdots,4; K \in \mathcal{K}^h\} \subset H_0^1(\Omega).$$

In the following, we study the approximate solution of (2.3) in V^h, i.e., to find $u^h \in V^h$ such that

$$a(u^h, v) = f(v), \quad \forall v \in V^h, \tag{2.6}$$

where u^h is the solution of the MFEM.

It is known that when the parameters ε_k are large, that is, $h \ll \varepsilon_k$, the MFEM behaves similarly as the FEM [13]. However, when ε_k are very small, that is, $\varepsilon_k \ll h$, the two methods behave differently. In this case, we make $h_s = h/M$ to satisfy $h_s \ll \varepsilon_k$. There are two ways for constructing the multiscale base functions: one is to do it in the original coarse element K directly, and the other one is to construct them with the over-sampling technique in larger coarse elements. The over-sampling technique for the multiscale finite element method can settle the resonance error [6, 12]. It is known that the resonance error is the strongest when $h = \varepsilon_k$, which is more visible for periodic coefficients and is generically small for random coefficients. In practice, such as flow simulation in a large region, the mesh size h is always larger than the physical small scale ε_k; thus there is no resonance existing. However, using the over-sampling technique to construct the base functions will increase the demand of computing resources. Therefore, in this paper we construct the base functions for the MFEM directly in the original coarse element with the linear and the oscillatory boundary condition, respectively.

3   Boundary condition of the base functions

The boundary condition in the local problem (2.5) for the base functions is very important; different boundary conditions can affect the accuracy and convergence of the MFEM scheme. Below we describe two different kinds of boundary conditions.

3.1   Linear boundary condition

We let θ^i vary linearly on ∂K, just like in the standard bilinear base functions. This is called linear boundary condition. For example, for base function ϕ^1 one has

$$\begin{aligned}
\theta^1(x) &= \frac{x_2 - x}{x_2 - x_1}, \quad x \in (x_1, x_2),\\
\theta^1(y) &= \frac{y_4 - y}{y_4 - y_1}, \quad y \in (y_1, y_4).
\end{aligned} \tag{3.1}$$

This kind of boundary condition was employed in [8, 13].

3.2 Oscillatory boundary condition

In this case, we solve the ordinary differential equations in each element on ∂K. These ODEs are obtained from (2.5) by deleting terms with partial derivatives in the direction normal to ∂K. When the multiscale coefficients are separable variables, i.e., the coefficients can be written as

$$a_{ij}\left(\frac{x}{\varepsilon_k},\frac{y}{\varepsilon_k}\right)=a_{ij}^1\left(\frac{x}{\varepsilon_k}\right)\cdot a_{ij}^2\left(\frac{y}{\varepsilon_k}\right). \tag{3.2}$$

In this case, we can derive

$$\frac{d}{dx}\left(a_{ij}^1\left(\frac{x}{\varepsilon_k}\right)\frac{d\theta^i(x)}{dx}\right)=0 \quad \text{on} \quad \partial K's \; x \; \text{direction}, \tag{3.3}$$

$$\frac{d}{dy}\left(a_{ij}^2\left(\frac{y}{\varepsilon_k}\right)\frac{d\theta^i(y)}{dy}\right)=0 \quad \text{on} \quad \partial K's \; y \; \text{direction}, \tag{3.4}$$

which can be solved analytically. For example, for base function ϕ^1 one has

$$\theta^1(x)=\int_x^{x_2}\frac{ds}{a_{ij}^1(s/\varepsilon_k)}\Big/\int_{x_1}^{x_2}\frac{ds}{a_{ij}^1(s/\varepsilon_k)}, \quad x\in(x_1,x_2),$$

$$\theta^1(y)=\int_y^{y_4}\frac{dt}{a_{ij}^2(t/\varepsilon_k)}\Big/\int_{y_1}^{y_4}\frac{dt}{a_{ij}^2(t/\varepsilon_k)}, \quad y\in(y_1,y_4). \tag{3.5}$$

The base functions ϕ^2, ϕ^3, ϕ^4 can be obtained similarly, It can be verified that if a_{ij} are constants, the oscillatory boundary condition becomes the linear boundary condition.

With either boundary condition, we solve the local problem (2.5) by the standard finite element method for the base functions. We will see in Section 4 that the oscillatory boundary condition (3.5) is better than the linear boundary condition (3.1) in many cases, but there exist some exceptions.

4　Numerical experiments

In this section, we investigate the accuracy and convergence of the multiscale finite element method using some numerical experiments. Since it is very difficult to construct a genuine two-dimensional multiscale problem with both exact solution and extensive generality, we use the resolved numerical solution to replace the exact solution. The resolved solution is obtained by using standard FEM on two fine mesh grids 1024×1024 and 2048×2048. Then the 'exact' solution u is obtained by using Richardson extrapolation technique to accelerate the accuracy on the two grids. Since both mesh sizes resolve the smallest scale among ε_k, the error of the extrapolation is acceptably very small.

The computations are carried out in a unit square domain $\Omega=(0,1)^2$ with rectangular meshes. We denote N the partition number in the x and y directions. Thus the domain Ω is divided into $N\times N$ elements with multiscale mesh size $h=1/N$. To compute the

Table 1: Example 4.1: the l_2-error and the convergence rate by MFEM(L) and MFEM(O) with $\varepsilon_1 = 0.2$ and $\varepsilon_2 = 0.08$. In this case, $u_{max} \approx 0.0263$.

ε_1	ε_2	N	M	$MFEM(L)$	$rate$	$MFEM(O)$	$rate$
0.2	0.08	32	8	1.107e-3		4.281e-5	
		64	8	3.642e-4	1.60	9.057e-6	2.24
		128	8	9.506e-5	1.94	2.797e-6	1.70
		256	8	2.451e-5	1.96	8.196e-7	1.77
		512	8	6.186e-6	1.99	2.150e-7	1.93

Table 2: Example 4.1: the l_2-error and the convergence rate by MFEM(L) and MFEM(O) with $\varepsilon_1 = 0.125$ and $\varepsilon_2 = 0.0078125$. In this case, $u_{max} \approx 0.0264$.

ε_1	ε_2	N	M	$MFEM(L)$	$rate$	$MFEM(O)$	$rate$
0.125	0.0078125	8	16	9.330e-3		1.034e-2	
		16	16	4.787e-3	0.96	5.429e-3	0.93
		32	16	1.538e-3	1.64	1.958e-3	1.47
		64	16	5.699e-4	1.43	3.092e-4	2.66
		128	16	1.558e-3	-1.45	2.340e-5	3.72

base functions in (2.5), each element is divided into $M \times M$ subelements with mesh size $h_s = h/M$.

We use the two boundary conditions described in Section 3. After using the standard FEM to solve the local problem for base functions, we compute the gradient of the base functions at the center of the subelements. The local stiffness matrix and the local rights-hand side in (2.4) are computed using the two-dimensional Gauss quadrature rule. Then we glue the local stiffness matrix to the global stiffness matrix. The resulting discrete algebra equations by using the algebraic multigrid method.

To analyze the error of the MFEM, we compare the MFEM solution u^h with the 'exact' solution approximation u. The same exact solution u is used for the MFEM with both the linear base functions (denoted by MFEM(L)) and the oscillatory base functions (denoted by MFEM(O)). In the following tables, the discrete l_2 norm errors are listed for the MFEM(L) and the MFEM(O), and the *rate* is the convergence rate when the grid is refined.

Example 4.1. We solve (2.1) with $f = 1$, $u|_{\partial\Omega} = g = 0$ and the periodic coefficient that

$$a_{ij} = \left(\frac{2 + 1.8\sin\left(\frac{2\pi x}{\varepsilon_1}\right)}{2 + 1.8\cos\left(\frac{2\pi y}{\varepsilon_2}\right)} + \frac{2 + 1.8\cos\left(\frac{2\pi y}{\varepsilon_1}\right)}{2 + 1.8\sin\left(\frac{2\pi x}{\varepsilon_2}\right)} \right) \cdot \delta_{ij}. \tag{4.1}$$
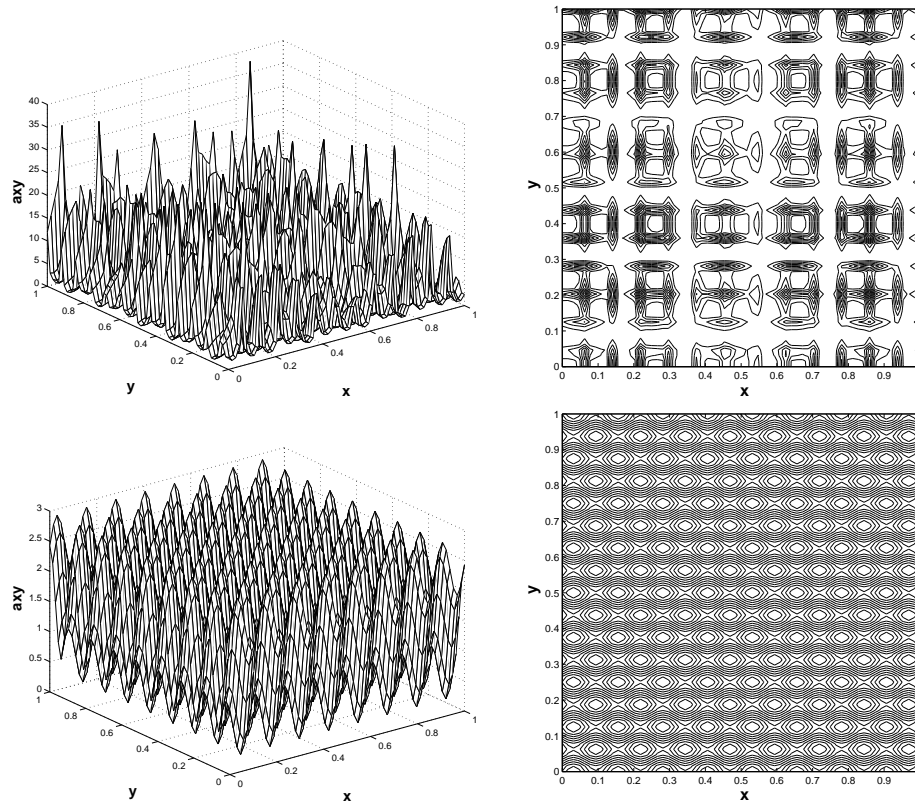
Figure 1: Example 4.1: the 3D view (left) and the 2D contour (right) for the coefficient function (4.1). Top: $\varepsilon_1 = 0.2, \varepsilon_2 = 0.08$, and the value of $\max(a)/\min(a)$ is 15.998; Bottom: $\varepsilon_1 = 0.125, \varepsilon_2 = 0.0078125$, the value of $\max(a)/\min(a)$ is 3.243.

In [8], it is proved that the error MFEM(L) satisfies

$$\text{for case } h \ll \varepsilon_2 \ll \varepsilon_1 : ||u - u^h||_{0,\Omega} \leq C \left(\frac{h}{\varepsilon_2} \right)^2, \tag{4.2}$$

$$\text{for case } \varepsilon_2 \ll h \ll \varepsilon_1 : ||u - u^h||_{0,\Omega} \leq C_1 \left(\frac{h}{\varepsilon_1} \right)^2 + C_2 \left(\frac{\varepsilon_2}{h} \right). \tag{4.3}$$

In Tables 1 and 2, different values of ε_1 and ε_2 are chosen, and the corresponding errors and the rate of convergence are shown. We also plot in Fig. 1 the 3D and 2D views of the coefficient function (4.1). It is seen from Fig. 1 that the periodic coefficient is parallel to the mesh grids. For the case $h \ll \varepsilon_2 \ll \varepsilon_1$, it is observed from Table 1 that the accuracy of MFEM(O) is much higher than that of MFEM(L). Moreover, both boundary conditions yield second-order rate of convergence, which verifies (4.2). For the case $\varepsilon_2 \ll h \ll \varepsilon_1$, it is observed from Table 2 that the rate of convergence for MFEM(L) deteriorates from second-order (when the term $(h/\varepsilon_1)^2$ dominates) to negative first-order (when the term
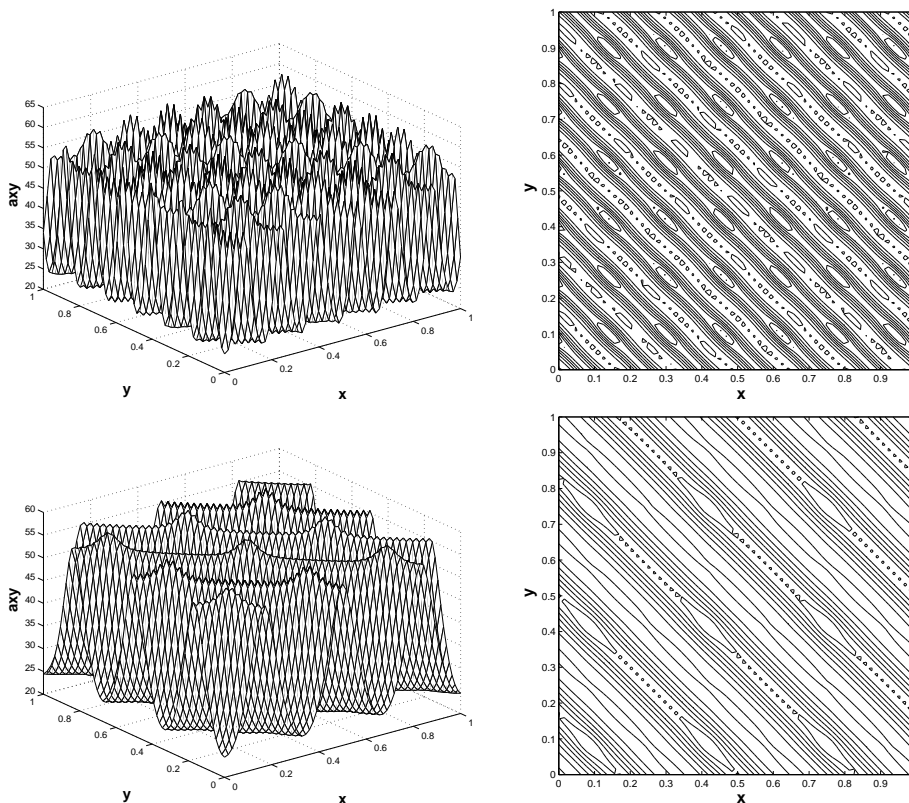
Figure 2: Example 4.2: the 3D view (left) and the 2D contour (right) for the coefficient function (4.4). Top: $\varepsilon_1 = 0.16$, and the value of $\max(a)/\min(a)$ is 2.288; Bottom: $\varepsilon_1 = 0.008$, the value of $\max(a)/\min(a)$ is 2.286.

ε_2/h dominates in (4.3)). In contrast, MFEM(O) can acquire high positive order convergence rate as the mesh is refined.

Example 4.2. We make coordinate transformation to periodic coefficient in this example. Solve (2.1) with $f = 1$ and $g = 0$, and

$$a_{ij} = \left(2 + 1.5\sin\left(\frac{2\pi(x+y)}{\varepsilon_1}\right)\right)^{-1}\left(2 + 1.5\sin\left(\frac{2\pi(x-y)}{\varepsilon_1}\right)\right)^{-1}\cdot\delta_{ij}. \tag{4.4}$$

In Fig. 2, we observe the coordinates transformation effects on the coefficient $a(\mathbf{x})$, where the coarse grid boundary edge cuts across the contours under irrational angle ($\pi/4$ in this example), which is different from Example 4.1.

It is observed from Table 3 that for case $h \ll \varepsilon_1$ both MFEM(L) and MFEM(O) obtain second-order convergence rate. However, the accuracy of MFEM(O) is lower than that of MFEM(L). Moreover, it is seen that for the case $h \gg \varepsilon_1$, the convergence rate for MFEM(L) deteriorates from second-order to negative first-order, while MFEM(O) is more accurate in this case. These phenomena were also noticed in Example 7.1 in [13]. It seems that

Table 3: Example 4.2: the l_2-error and the convergence rate by MFEM(L) and MFEM(O) with $\varepsilon_1 = 0.16$. In this case, $u_{\max} \approx 0.19393$.

ε_1	N	M	MFEM(L)	rate	MFEM(O)	rate
0.16	32	8	1.609e-3		4.259e-3	
	64	8	3.562e-4	2.18	1.577e-3	1.43
	128	8	8.627e-5	2.05	4.498e-4	1.81
	256	8	2.142e-5	2.01	1.168e-4	1.95
	512	8	5.352e-6	2.00	2.950e-5	1.99

when the boundary edge of the coarse elements cuts through the contours of the periodic coefficient under irrational angle, MFEM(O) with large parameter $\varepsilon_1 = 0.16$ (as in Table 3) can not extract more accurate information on the boundary. On the contrary, MFEM(O) with small parameter $\varepsilon_1 = 0.008$ can behave better. This is because when the boundary edge goes through the entire period due to ergodicity as $\varepsilon_k \to 0$, sufficient information is to be captured by the oscillatory multiscale base functions.
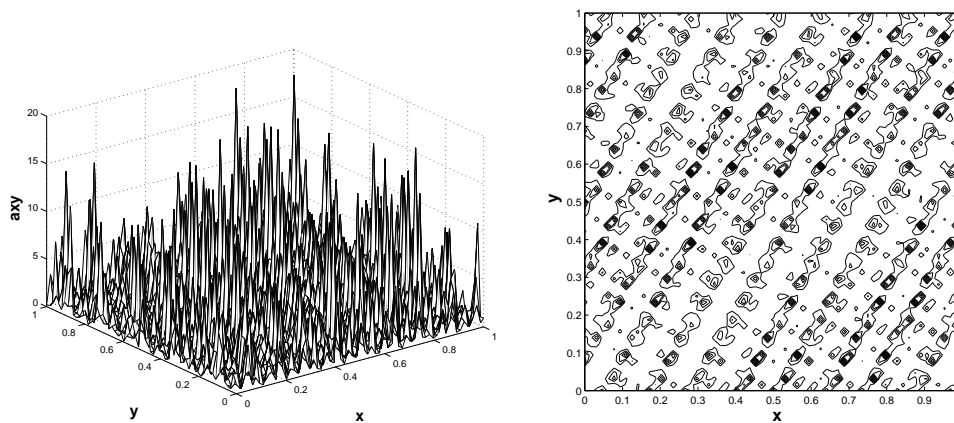
Figure 3: Example 4.3: the 3D view (left) and the 2D contour (right) for the coefficient function (4.5), with $\varepsilon_1 = 0.2, \varepsilon_2 = 0.08$. The value of $\max(a)/\min(a)$ is 148.444.

Example 4.3. We make another coordinate transformation to periodic coefficient. Solve (2.1) with $f = 1$, $u|_{\partial\Omega} = g = 0.5(x^2 + y^2)$, and

$$a_{ij} = \left(\frac{1.5 + \sin\left(\frac{2\pi(\sqrt{3}x + 3y)}{\varepsilon_1}\right)}{1.5 + \cos\left(\frac{2\pi(\sqrt{3}x - y)}{\varepsilon_1}\right)} \cdot \frac{1.5 + \cos\left(\frac{2\pi(\sqrt{3}x - y)}{\varepsilon_2}\right)}{1.5 + \sin\left(\frac{2\pi(\sqrt{3}x + 3y)}{\varepsilon_2}\right)} \right) \cdot \delta_{ij}. \tag{4.5}$$

Fig. 3 presents the 3D view and the 2D contour for $a(\mathbf{x})$. It is seen that the mesh grid goes through the contours of the coefficient under irrational angle ($\pi/3$ in this example).

Table 4: Example 4.3: the l_2-error and the convergence rate by MFEM(L) and MFEM(O) with $\varepsilon_1 = 0.2$ and $\varepsilon_2 = 0.08$. In this case, $u_{\max} = 1$.

ε_1	ε_2	N	M	$MFEM(L)$	$rate$	$MFEM(O)$	$rate$
0.2	0.08	64	8	3.748e-3		1.821e-3	
		128	8	8.610e-4	2.12	9.102e-4	1.00
		256	8	2.035e-4	2.08	3.197e-4	1.51
		512	8	5.094e-5	2.00	8.994e-5	1.83

It is seen from Table 4 that for case $h \ll \varepsilon_2 \ll \varepsilon_1$, MFEM($L$) is a little more accurate than MFEM(O). For the case $\varepsilon_2 \ll h \ll \varepsilon_1$, it is found that there is no big difference in accuracy between MFEM(L) and MFEM(O).

From Examples 4.2 and 4.3, we remark that in the situation that the mesh element edge cuts through the contours of the periodic coefficient under irrational angle, there is no great difference using either the linear or oscillatory boundary condition for the multiscale bases when small scales present; however, it should be pointed out when there are large scale parameters, MFEM(L) behaves better than MFEM(O) in this case.
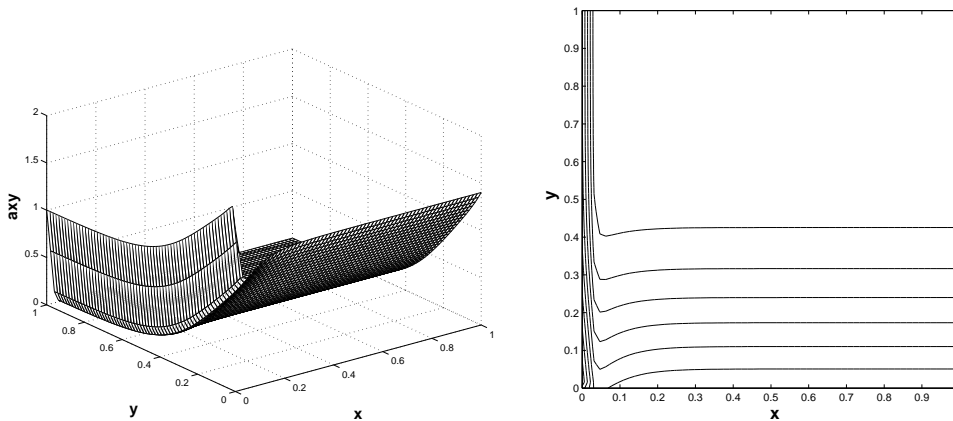

Figure 4: Example 4.4: the 3D view (left) and the 2D contour (right) for the coefficient function (4.6), with $\varepsilon_1 = 0.125, \varepsilon_2 = 0.0078125$, and the value of $\max(a)/\min(a)$ is 2.384.

Example 4.4. The last example is concerned with the non-periodic coefficient in (2.1):

$$a_{ij} = \left(\frac{2.5 + \tanh(x/\varepsilon_1)}{2.5 + \sinh(y/\varepsilon_1)} + \frac{2.5 + \tanh(y/\varepsilon_2)}{2.5 + \cosh(x/\varepsilon_2)} \right) \cdot \delta_{ij}, \tag{4.6}$$

together with $f = 1, g = x$.

For the non-periodic coefficient situation, the contours in Fig. 4 have no regularity with the mesh grid boundary. In Table 5, for the case $h \ll \varepsilon_2 \ll \varepsilon_1$, MFEM($L$) and MFEM($O$) behave similarly and the second-order convergence rate is not in this case. In Table 6, for

Table 5: Example 4.4: the l_2-error and the convergence rate by MFEM(L) and MFEM(O) with $\varepsilon_1 = 0.2$ and $\varepsilon_2 = 0.08$. In this case, $u_{\max} \approx 1.023$.

ε_1	ε_2	N	M	$MFEM(L)$	$rate$	$MFEM(O)$	$rate$
0.2	0.08	32	8	8.123e-5		1.296e-4	
		64	8	2.158e-5	1.91	3.403e-5	1.93
		128	8	7.007e-6	1.62	1.016e-5	1.74
		256	8	4.106e-6	0.77	4.779e-6	1.09
		512	8	3.655e-6	0.17	3.792e-6	0.33

Table 6: Example 4.4: the l_2-error and the convergence rate by MFEM(L) and MFEM(O) with $\varepsilon_1 = 0.125$ and $\varepsilon_2 = 0.0078125$. In this case, $u_{\max} \approx 2.895$.

ε_1	ε_2	N	M	$MFEM(L)$	$rate$	$MFEM(O)$	$rate$
0.125	0.0078125	8	16	1.167e-1		2.086e-2	
		16	16	2.964e-2	1.98	6.146e-3	1.76
		32	16	7.976e-3	1.89	1.606e-3	1.94
		64	16	1.908e-3	2.06	4.069e-4	1.98
		128	16	4.867e-4	1.97	1.027e-4	1.99

the case $\varepsilon_2 \ll h \ll \varepsilon_1$, the numerical results obtained by using MFEM(O) are more accurate than those of MFEM(L). This is due to the well-being of the ergodicity refined by the small parameters. So we conclude that in the non-periodic situation, MFEM(O) is a good choice for the multiscale problem.

5 Conclusions

Through numerical studies on the boundary conditions of the base functions for the multiscale finite element method, we demonstrate the superiority of the oscillatory boundary condition for the multiscale base functions in many cases. However, the oscillatory boundary condition is not a *panacea* in all cases. It is observed that when the boundary edge of the coarse grids cuts through the contours of the coefficient under irrational angle, the large scale parameters will affect the well-being of the ergodicity. Consequently, the ill-fitted of the oscillatory boundary condition may yield less accurate results than those given by the linear boundary condition.

Acknowledgments

referees for their insightful comments and helpful suggestions, which led to a significant improvement of the paper.

References

[1] I. Babuška, G. Caloz and E. Osborn, Special finite element methods for a class of second order elliptic problems with rough coefficients, SIAM J. Numer. Anal., 31(1994), 945-981.

[2] I. Babuška and E. Osborn, Generalized finite element methods: Their performance and their relation to mixed methods, SIAM J. Numer. Anal., 20(1983), 510-536.

[3] J. Bear, Use of models in decision making, Transport and Reactive Processes in Aquifers, Balkema, Rotterdam, (1994), 3-9.

[4] J. R. Chen and J. Z. Cui, A multiscale rectangular element method for elliptic problems with entirely small periodic coefficients, Appl. Math. Comput., 130(2002), 39-52.

[5] Z. M. Chen and T. Y. Hou, A mixed multiscale finite element method for elliptic problems with oscillating coefficients, Math. Comput., 72(2002), 541-576.

[6] Z. M. Chen and X. Y. Yue, Numerical homogenization of well singularities in the flow transport through heterogeneous porous media, Multiscale Model. Sim., 1(2003), 260-303.

[7] Y. Efendiev and T. Y. Hou, Multiscale finite element methods for porous media flows and their applications, Appl. Numer. Math., 57(2007), 577-596.

[8] Y. Efendiev and X. H. Wu, Multiscale finite element for problems with highly oscillatory coefficients, Numer. Math., 90(2002), 459-486.

[9] B. Engquist and E. Luo, Convergence of a multigrid method for elliptic equations with highly oscillatory coefficients, SIAM J. Numer. Anal., 34(1997):2254-2273.

[10] W. E, B. Engquist, X. T. Li, W. Ren, E. Vanden-Eijnden, Heterogeneous multiscale methods: A review, Commun. Comput. Phys., 2(2007), 367-450.

[11] X. G. He and L. Ren, Finite volume multiscale finite element method for solving the groundwater flow problems in heterogeneous porous media, Water Resour. Res., 41(2005), W10417, doi:10.1029/2004WR003934.

[12] T. Y. Hou and X. H. Wu, A multiscale finite element method for elliptic problems in composite materials and porous media, J. Comput. Phys., 134(1997), 168-189.

[13] T. Y. Hou, X. H. Wu and Z. Cai, Convergence of a multiscale finite element method for elliptic problems with rapidly oscillating coefficients, Math. Comput., 68(1999), 913-943.

[14] Y. Q. Huang and J. Xu, A partition of unity finite element method for elliptic problems with highly oscillating coefficients, in Proceedings for the Workshop on Scientific Computing, Hong Kong, (1999).

[15] Y. Q. Huang and J. Xu, A conforming finite element method for overlapping and nonmatching grids, Math. Comput., 72(2002), 1057-1066.

[16] P. Jenny, S. H. Lee and H. A. Tchelepi, Multiscale finite-volume method for elliptic problems in subsurface flow simulation, J. Comput. Phys., 187(2003), 47-67.

[17] P. B. Ming and X. Y. Yue, Numerical methods for multiscale elliptic problems, J. Comput. Phys., 214(2006), 421-445.

[18] V. Nassehi, M. Parvazinia and A. Khan, Multiscale finite element modelling of flow through porous media with curved and contracting boundaries to evaluate different types of bubble functions, Commun. Comput. Phys., 2(2007), 723-745.

[19] W. Q. Ren and W. E, Heterogeneous multiscale method for the modeling of complex fluids and micro-fludics, J. Comput. Phys., 204(2005), 1-26.

[20] X. Y. Yue and W. E, Numerical methods for multiscale transport equations and application to two-phase porous media flow, J. Comput. Phys., 210(2005), 656-675.
[21] X. Y. Yue and W. E, The local microscale problem in the multiscale modeling of strongly heterogeneous media: Effects of boundary conditions and cell size, J. Comput. Phys., 222(2007), 556-572.